International Journal of Robotics and Automation, Vol. 36, 2021

Special Issue: Artificial Intelligence in Environmental Automation Systems

VEGETATION CLASSIFICATION BY MULTI-SCALE HIERARCHICAL SEGMENTATION ON GF-2 REMOTE SENSING IMAGE

Yang Wugu,* Tian Weixin,*,** and Ming Lei*

Abstract

Further classifying the vegetation into subclasses is significant for some applications such as ecological protection and vegetation mapping. A method based on multi-scale segmentation is proposed in this paper to separate the GF-2 remote sensing image into objects on different hierarchies. On each layer, high-resolution images are separated by using spectral, shape, texture and other image features. Experiment on the data of area along the Yangtze River in the Dianjun District of Yichang City shows the efficiency of the method. When the shape factor fixed to 0.1 and three layers used with fuzzy membership classifier and k-nearest neighbour classifier, respectively, the kappa coefficient of the final vegetation classification reaches 0.97.

Key Words

Remote sensing, vegetation classification, multi-scale segmentation, hierarchical segmentation

1. Introduction

With the growing source of high-resolution remote sensing image, the application of remote sensing images is increasing [1]. Compared with manual survey, the application of remote sensing technology greatly improves the accuracy and efficiency. Vegetation is an important component of the ecosystem. Accurate extraction of surface vegetation coverage is one of the key tasks of global ecological environmental protection [2].

In recent years, the classification of remote sensing images is mainly based on the method of clustering and threshold segmentation, such as the application of fuzzy c-means clustering [3], K-means clustering [4] and mean shift clustering [5]–[8]. While in the threshold segmentation, the threshold is set to the minimal value on the grey histogram between the peaks of foreground and background. The threshold segmentation got good results in the binary classification on medium- and low-resolution remote sensing images. For high-resolution remote sensing images, relatively more noise is generated, which reduces the accuracy of classification.

Object-oriented classification can solve the noise problem. Image segmentation is one of the key steps in object-oriented classification [9], [10]. The final goal of segmentation algorithm is to separate different categories of objects. Multi-scale segmentation can achieve results consistent with the human eyes by using regional growing and local optimal segmentation strategies. However, the accuracy is heavily affected by the segmentation parameters and scales, which is hard to tune. By using hierarchical strategy, good accuracy of multi-scale segmentation can be achieved and will be less impacted by the scales [11].

Hierarchical strategy can make full use of the advantage of multi-scale segmentation and reduce the influence of complexity of ground objects on the overall classification quality, in which different scales are selected hierarchically and classification rules are designed according to the target objects at each layer. Because the segmentation object of high-resolution remote sensing image contains more information than that of low resolution, it is necessary to adopt different segmentation scales for different ground objects hierarchically. Meanwhile, due to the feature complexity of segmentation objects, the classification of remote sensing images in different regions has a large error under the same segmentation scale. Therefore, in practical application, it is necessary to customize segmentation parameters and scale according to specific research area and image features, and conduct segmentation hierarchically in combination with scale evaluation algorithm, and then further complete the classification of specific research area [12]–[14].

Vegetation classification mainly consists of two steps: extraction of vegetation and accurate segmentation of various vegetation categories. Object-oriented methods are

* Hubei Engineering Technology Research Center for Farmland Environmental Monitoring, China Three Gorges University, Yichang 443002, China; e-mail: t_wxin@126.com

** Comupter and Information Technology School, China Three Gorges University, Yichang 443002, China

Corresponding author: Tian Weixin

Recommended by Dr. Dong Ren

(DOI: 10.2316/J.2021.206-0617)

used combining features to address this task on high-spatial-resolution remote sensing images on the basis of different scales [15]–[17]. This study is based on GF-2 remote sensing image, which is of high spare resolution with four bands. The images are segmented in different scales hierarchically. The estimation of scale parameter 2 (ESP2) tool is used to find the local optimal scale. At the first layer, when the near-infrared band average is greater than 156 and the normalized difference water index (NDWI) is <0.28, the non-water body is extracted. The vegetation is separated from the non-water body at the second layer when the normalized difference vegetation index (NDVI) is >0.12. After using the fuzzy membership classification [18] of the first two layers, the third layer further uses the k-nearest neighbour (KNN) classifier [19] to refine the vegetation classification. The kappa coefficient of vegetation classification results can reach 0.97 in Dianjun District of Yichang City along the Yangtze River.

2. Research Area and Data Source

The research area of this study locates on the Dianjun District of Yichang City, Hubei Province, near the bank of Yangtze River. There are mainly mountains and hills in the area. The main type of the land cover in the area is forest land, and there are also small number of residential areas, water bodies and roads. The location of the research area is shown in Fig. 1.

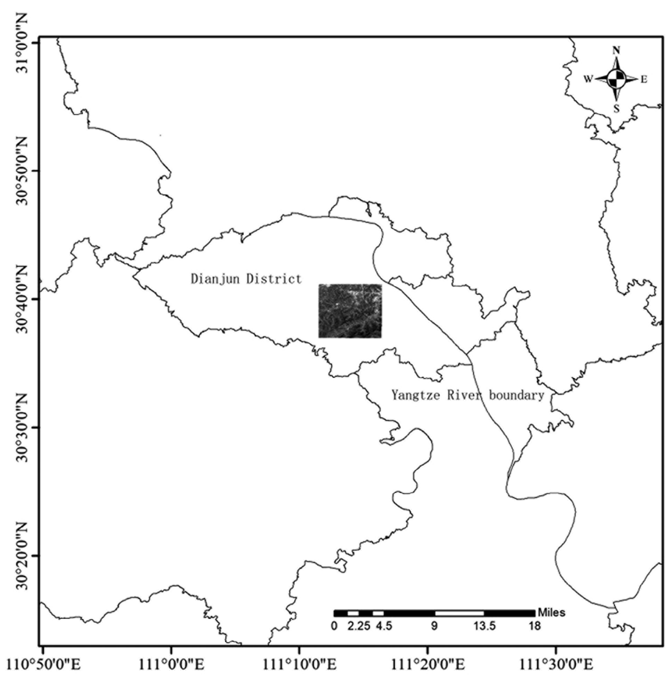

Figure 1. The location of the research area.

The remote sensing image used in this study is taken by GF-2 on 13 April 2015. The longitude and latitude of the image ranges from 111°11′E to 111°16′E and 30°37′N to 30°41′N, respectively. The size of original multi-spectral image is 2000×2000 pixels.

GF-2 satellite is the first civil optical remote sensing satellite independently developed by China with a spatial resolution better than 1 m. It was put into use in March 2015. GF-2 takes both panchromatic images and multi-spectral images, while panchromatic images have a resolution of 1 m and multi-spectral images have a resolution of 3.9 m. Furthermore, multi-spectral images contain four bands of R,G,B and near-infrared band. The wavelength information is presented in Table 1.

Table 1
GF-2 Image Bands Information

Band Order	Wavelength (nm)	Description
1	450–520	Blue
2	520–590	Green
3	630–690	Red
4	770–890	Near-infrared

The GF-2 image data used in this study is level 1A. Six pre-processing steps such as RPC orthorectification, registration, atmospheric correction,fusion, cropping and mosaic are done in ENVI 5.3. In the fusion step, Gram-Schmidt pan-sharpening fusion method is used to obtain multi-spectral images and panchromatic band images fusion data of the GF-2, which ensures the integrity of the spectral information of the image. After the fusion, the image size was 7800×7800 pixels.

3. Experiments

3.1 Object-Oriented Multi-Scale Segmentation

Image segmentation is to divide the image into several non-overlapping regions. Multi-scale segmentation ensures the highest homogeneity of the lowest heterogeneity of image objects. A data-driven method named fractal net evolution approach [20]–[24] is used in this stage. Starting from a single pixel, using a bottom-up approach to region aggregation, the image is segmented into entity objects with similar image features of different scales and sizes. Then the entity objects are used as units and classified according to various image feature parameters values.

The segmentation scale indicates the threshold for the smallest heterogeneity of the segmented object. If the scale is too large, the smaller object will be submerged, and if the scale is too small, the object will be broken. The selected scale should ensure that the regional object obtained after segmentation is in good agreement with the desired target. The heterogeneity of the object is calculated according to the spectral heterogeneity and shape heterogeneity of different weights. The calculation formula is given as:

$$f = w_1 x + (1 - w_1) y \tag{1}$$

where w_1 is weight, the value of which is between 0 and 1, x is spectral heterogeneity and y is shape heterogeneity.

Table 2
Object-Oriented Classification Features

Data Layer	Target Index	Index Number
Blue	Average grey value, standard deviation, brightness	3
Green	Average grey value, standard deviation, brightness, NDWI, the standard deviation and mean of grey-level co-occurrence matrix in green band	5
Red	Average grey value, standard deviation, brightness, NDVI, the standard deviation and mean of grey-level co-occurrence matrix in red band	5
Near-infrared	Average grey value, standard deviation, brightness	3 7

1. The shape heterogeneity of object is determined by two indicators: smoothness index and compactness index. Both indicators are used to measure the degree of regularity of the object, the weight of the smoothness index is high and the boundary of the divided object is relatively smooth; otherwise, if the weight of the compactness index is high, the shape of the segmented object is close to the rectangle. The shape heterogeneity of objects is the weighted average of the two index increments before and after merging. The expression is given as:

$$x = w_{smoothness} \times h_{smoothness} + w_{compactness} \times h_{compactness} \quad (2)$$

The sum of the weights of the two indicators is 1, according to different needs, adjust the weight proportion, and control the shape of the segmented object.

2. The spectral heterogeneity of a single object is the weighted average of the corresponding standard deviations of each band, which is used to measure the overall difference. The expression is given as:

$$y = \sum_c w_c \sigma_c \quad (3)$$

where w_c is the weight of different bands and σ_c is the standard deviation of the spectral values for the different bands.

When the adjacent image regions are merged, the regional local heterogeneity index is smaller than the threshold defined by the scale parameter. In practice, the segmentation scale of the image and the selection of the segmentation parameters at each scale need to be obtained through repeated experiments according to the characteristics of different feature images. On the basis of the characteristics of the image mentioned in Table 2, such as spectral characteristics and vegetation index characteristics, this study uses the ESP2 segmentation scale evaluation algorithm to find the optimal scale, and the experiments are carried out with the small study area image which contains relatively rich ground objects. The optimal scale of the segmentation of the large image and the small image is the same [25]. Intercept the size of 1000×1000 pixels, select three scales and divide the research area into three layers, according to the research of Peirong et al. [26], the shape factor is set to 0.1, the compactness is 0.9, the scale of the first layer is 300, the scale of the second layer is 200 and the scale of the third layer is 100. The segmentation effect of different scales is shown in Fig. 2.

3.2 Segmentation Scale Evaluation

This study uses the improved version ESP2 of the 2010 segmentation evaluation algorithm ESP by Drăguţ et al. in 2014. Compared with ESP, ESP2 improves the effect of changing the scale growth step size on the result, and can perform local variance (LV) traversal calculation on the whole image, which effectively reduces the estimated deviation of the segmentation parameters and scales, reflecting the total degree of discretization between the grey value of

(a) (b) (c)

Figure 2. Image multi-scale segmentation results: (a) level 1; (b) level 2; and (c) level 3.

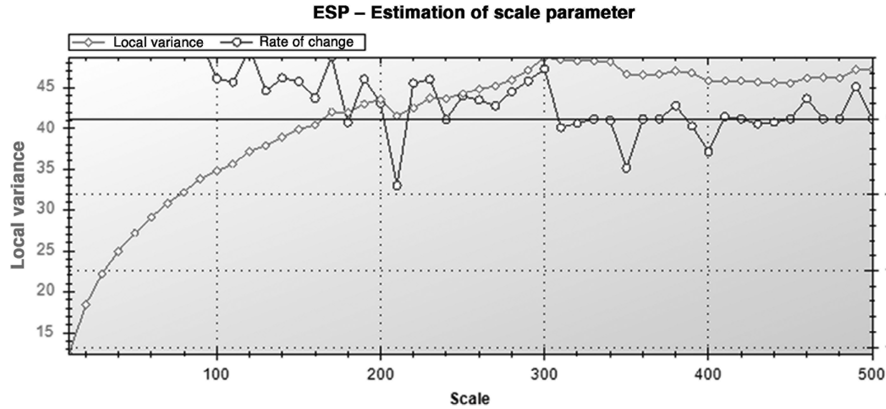

Figure 3. Segmentation scale evaluation.

each pixel and the average grey level of the local window. The calculation formula of the LV is given as:

$$LV(i,j) = \sqrt{\frac{\sum_{i=0}^{n}\sum_{j=0}^{n}[f(i,j) - f]^2}{n^2}} \tag{4}$$

where n is the window size, i, j is the number of rows and rows in the local window, $f(i,j)$ is the grey scale of the pixel in the local window and f is the grey mean value of the local window.

The local heterogeneity is reflected by the value of the LV, which reflects the overall dispersion degree of the grey value of each pixel and the average grey level of the local window. There is heterogeneity within the segmented image objects. When the remote sensing image data in the study area is large, there is no absolute optimal scale. It is feasible to find a locally relatively optimal scale for different levels of classification. In this paper, the parameter setting adopts the multi-level process bottom-up region growth method, the larger the shape index is, the more discrete the spatial morphological distribution is, and the greater the compactness is, the more irregular the object is. After comparison according that the shape factor is fixed at 0.1, the compactness is fixed at 0.9, the cycle number, the starting scale and the growth step size of each layer are set, and LV figure is generated, when the local heterogeneity takes the peak, the corresponding optimal segmentation scale is obtained. As shown in Fig. 3, when the scale value is 300, the local heterogeneity reaches a peak, which is applied to the pre-classification segmentation of the first layer with the best effect.

3.3 Classification

Object-oriented hierarchical classification is divided into three steps:

1. Create objects by image segmentation algorithm, and this paper adopts multi-scale segmentation;
2. Extracting features based on objects;
3. Classification based on classification features.

The KNN classification algorithm, that is k-nearest neighbour classification, a classification method mainly studied at level 3, is a theoretically mature method, a kind of machine learning algorithm. If the majority of the k most similar samples in a feature space belong to a certain category, the sample also belongs to this category. According to the marginality and clustering of this principle, this classification algorithm is suitable for object-oriented classification. This paper is based on multi-scale segmentation combined with this classification algorithm for object-oriented classification.

After image segmentation, the classification rules are established according to the spectral mean, NDVI, NDWI, shape index and texture features of the object, as shown in Fig. 4. The fuzzy membership function classifier is used to complete the classification of the vegetation and non-vegetation, water and non-water bodies.

By using the above fuzzy classification, the vegetation, water body and other three categories are separated, and then the nearest neighbour feature space is configured for the training sample by using the KNN classification method, including the spectral characteristics of the four bands, namely the mean value, standard deviation and the brightness, at the same time adding the texture features of the green band and the red band, *i.e.*, the grey level co-occurrence matrix as a supplementary feature, the characteristics used in the classification are presented in Table 2. Vegetation is divided into forest, plough, grassland and shallow forest using the KNN classifier. Among them, 100 objects of forest, 50 objects of plough, 10 objects of grassland and shallow forest were selected for the training samples, and the classification structure and category colour are shown in Fig. 5.

4. Result and Evaluation

Through the above multi-scale hierarchical segmentation method, the research area is divided into water, other, forest, plough, grass and shallow forest according to the above classification rules and classification structure. There are five categories, and the classification results are shown in Fig. 6. To evaluate its accuracy, this study randomly and automatically selects test samples, establishes confusing matrix and evaluates the accuracy of classification results, as presented in Table 3.

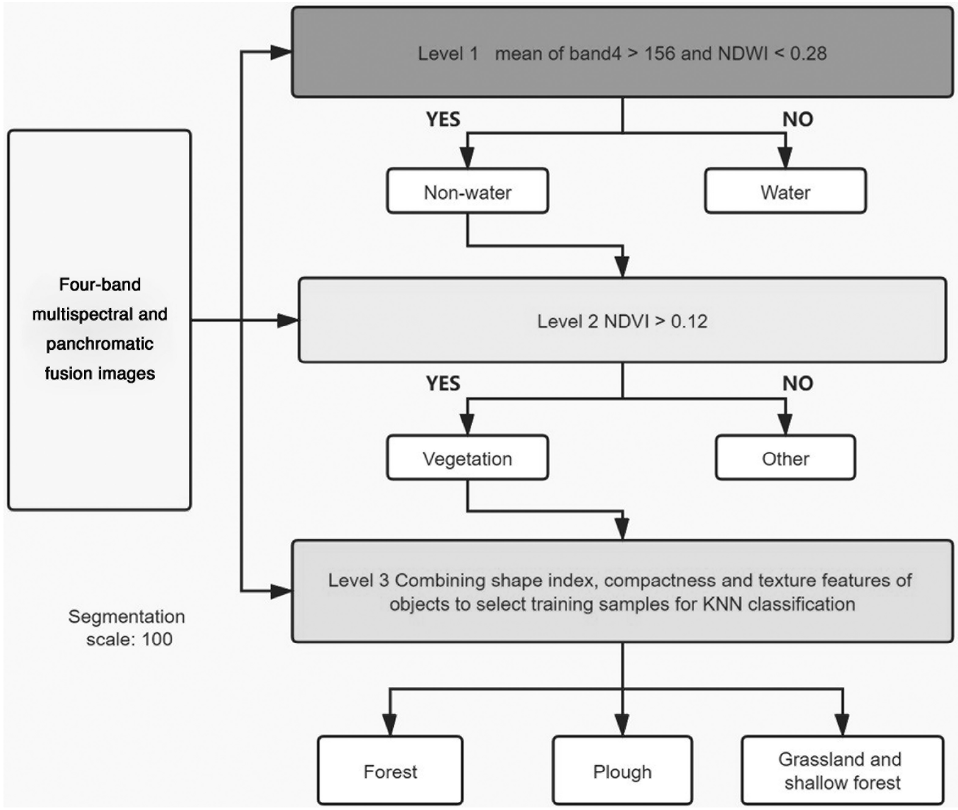

Figure 4. Classification rule map.

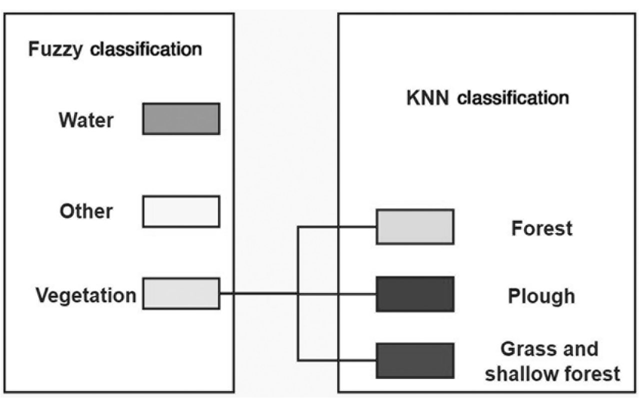

Figure 5. Classification structure.

Select Kappa coefficient combined with overall accuracy as the evaluation index of classification results [27]. The overall classification accuracy indicates the ratio of the number of categories correctly classified to the total number of categories.

The formula for calculating the Kappa coefficient:

$$K = \frac{N\sum_{i=1}^{m} x_{ii} - \sum_{i=1}^{n}(x_{i+}x_{+i})}{N^2 - \sum_{i=1}^{n}(x_{i+}x_{+i})} \tag{5}$$

where m is the number of rows in the error matrix, x_{ii} is the number of pixels in row i and column i, the number

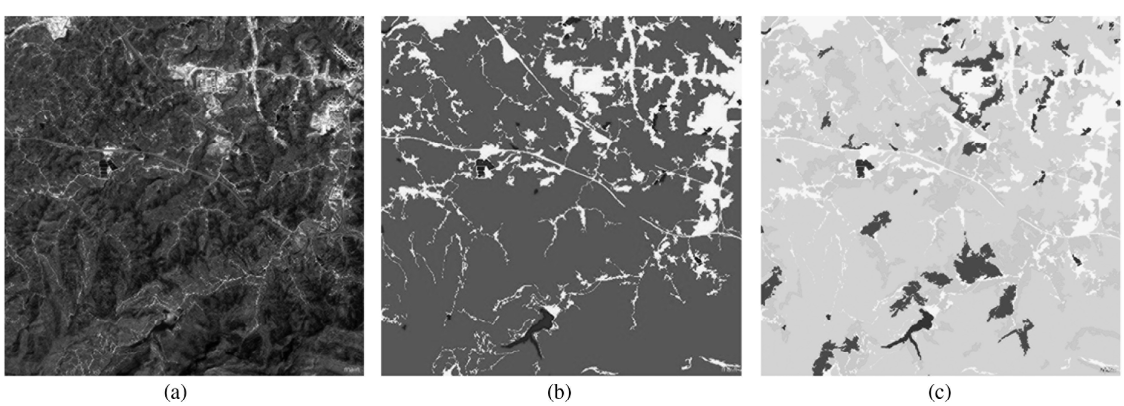

Figure 6. Fusion image (a), fuzzy classification result (b) and refined classification result (c).

Table 3
Comparison on Different Levels of Classification Results

Scale	Level 1	Level 2	Level 3	Kappa
Unlayered		300		0.77
Divided into two layers	300	200	300	0.79
		100	300	0.79
		300	200	0.86
		300	100	0.95
Divided into three layers	300	100	200	0.87
		200	100	0.97

Table 4
Comparison based on Different Classification Methods

Classification methods	Kappa coefficient	
	Unlayered	Layered
Neural network classification	0.81	0.93
Maximum likelihood classification	0.90	0.90
KNN classification	0.77	0.97

Table 5
Accuracy Evaluation of Multi-Scale Classification Results

Classification	Number of Test Samples					
	Water	Other	Plough	Grass and	Forest Shallow Forest	Sum
Water	9	0	0	0	0	9
Other	0	79	0	0	0	79
Plough	0	0	65	0	0	65
Forest	0	0	0	183	0	183
Grass and shallow forest	0	0	4	11	29	44
Sum	9	79	69	194	29	380
Producer accuracy	1	1	0.94	0.94	1	
User accuracy	1	1	1	1	0.66	
The overall accuracy: 0.96						

of correctly classified on the main diagonal, n is the total number of categories, x_{i+} is the total number of pixels in row i, x_{+i} is the total number of pixels in column i and N is the total number of pixels used for accuracy evaluation.

The study based on different features only focuses on the overall classification accuracy and the Kappa coefficient. The larger the two values, the better the classification effect. To improve the credibility of the results evaluation, the accuracy test of the image uses the same set of pixel-based test samples (TTAMask) to analyse the impact of multi-scale and hierarchical strategies on the classification results, as presented in Table 3, the comparison on the basis of different classification methods is presented in Table 4 and the detailed accuracy evaluation results of the best hierarchical classification is presented in Table 5.

5. Conclusion

In this study, the high-resolution remote sensing image GF-2 is used as the data source. On the basis of the multi-scale hierarchical segmentation, the object-oriented classification of remote sensing images in the Dianjun District of Yichang City is carried out. Take the segmented object as the unit, combined with the spectral features, texture features and shape index of the image, the KNN classifier is used to extract different vegetation types after the using of fuzzy membership classification on the first two layers, and good classification accuracy is obtained.

As there is no absolute overall optimal scale, this paper adopts the hierarchical classification strategy, combined with the reference of the segmentation parameters by eCognition software itself, and uses the ESP2 tool to calculate a theoretical local relative optimal scale for the sub-region extracted from the image. After then, combined with the local optimal scale value, different segmentation scales are used hierarchically, the integrated use of supervised and unsupervised classification improves the classification effect obviously for vegetation information extraction along the Yangtze River in Yichang City.

Acknowledgement

This work was supported in part by the National Key Research and Development Projects of China (Grant No. 2016YFD0800902) and Major Technological Innovation Project in Hubei Province of China (Grant No. 2017ABA157).

References

[1] X. Huang and L. Zhang, An SVM ensemble approach combining spectral, structural, and semantic features for the classification of high-resolution remotely sensed imagery, *IEEE Transactions on Geoscience and Remote Sensing*, *51*(1), 2013, 257–272.

[2] S. Dzikitia, M.B. Gusha, D.C. Le Maitrea, A. Maherrya, N.Z. Jovanovica. A. Ramoeloab, *et al.*, Quantifying potential water savings from clearing invasive alien *Eucalyptus camaldulensis* using in situ and high resolution remote sensing data in the Berg River Catchment, Western Cape, South Africa, *Forest Ecology and Management*, *361*, 2016, 69–80.

[3] H. Hongyuan, G. Jifa, and L. Zhao-Liang, Hyperspectral image classification for land cover based on an improved interval type-II fuzzy *c*-means approach, *Sensors*, *18*(2), 2018, 363–376.

[4] J. Tao, H. Dan, and Y. Xianchuan, Enhanced FCM algorithm using object-based triangular fuzzy set modeling for remote-sensing clustering, *Computers & Geosciences*, *118*, 2018, 14–26.

[5] M. Dongping, C. Tianyu, C. Hongyue, L. Longxiang, Q. Cheng, and D. Jinyang, Semivariogram-based spatial bandwidth selection for remote sensing image segmentation with mean-shift

algorithm, *IEEE Geoscience and Remote Sensing Letters*, *9*(5), 2012, 813–817.

[6] J. Michel, D. Youssefi, and M. Grizonnet, Stable mean-shift algorithm and its application to the segmentation of arbitrarily large remote sensing images, *IEEE Transactions on Geoscience and Remote Sensing*, *53*(2), 2015, 952–964.

[7] W. Tianjun, X. Liegang, L. Jiancheng, Z. Xiaocheng, H. Xiaodong, M. Jianghong, *et al.*, Computationally efficient mean-shift parallel segmentation algorithm for high-resolution remote sensing images, *Journal of the Indian Society of Remote Sensing*, *46*(11), 2018, 1805–1814.

[8] S. Tengfei, Z. Shengwei, and L. Hongyu, Variable scale mean-shift based method for cropland segmentation from high spatial resolution remote sensing images, *Remote Sensing for Land & Resources*, *29*(3), 2017, 118–123.

[9] R. Dong, Z. Chang, R. Shun, Z. Zhong, W. Jihua, and L. Anxiang, An improved approach of cars for Longjing tea detection based on near infrared spectra, *International Journal of Robotics & Automation*, *33*(1), 2018, 97–103.

[10] P. Shao, W. Shi, and M. Hao, Indicator-kriging-integrated evidence theory for unsupervised change detection in remotely sensed imagery, *IEEE Journal of Selected Topics in Applied Earth Observations and Remote Sensing*, *11*(12), 2018, 4649–4663.

[11] M. Xuegang, D. Zihan, L. Jiaqian, C. Shuxin, and H. Jiyu, Object-oriented segmentation and classification of forest gap based on Quick Bird remote sensing image, *Chinese Journal of Applied Ecology*, *29*(1), 2018, 44–52.

[12] M. Belgiu and L. Drăguţ, Random forest in remote sensing: A review of applications and future directions, *ISPRS Journal of Photogrammetry & Remote Sensing*, *114*, 2016, 24–31.

[13] Z. Hua and Z. Gaichang, Multi-scale segmentation of object-oriented GF-1 remote sensing image, *Journal of Gansu Agricultural University*, *53*(4), 2018, 116–123.

[14] T. Zhou, L. Gu, and R. Ren, Application of multi-scale segmentation algorithms for high resolution remote sensing image, *Applications of Digital Image Processing XL*, San Diego, California, United States, 2017.103961T

[15] M. Xuegang, D. Zihan, L. Jiaqian, C. Shuxin, and H. Jiyu, Segmentation and classification of QuickBird remote sensing image based on object-oriented segmentation, *Chinese Journal of Applied Ecology*, *29*(1), 2018, 44–52.

[16] Y. Ma, D. Ming, and H. Yang, Scale estimation of object-oriented image analysis based on spectral-spatial statistics, *Journal of Remote Sensing*, *21*(4), 2017, 566–578.

[17] L. Xiaodan, Y. Ning, and Q. Hongyuan, Hierarchical multi-scale vegetation segmentation of remote sensing image based on spectral histogram, *Remote Sensing of Land and Resources*, *29*(2), 2017, 82–89.

[18] W. Chunyan, L. Jiaxin, X. Aigong, W. Yu, and S. Xin, A new method of fuzzy supervised classification of high resolution remote sensing image, *Geomatics & Information Science of Wuhan University*, *43*(6), 2018, 922–929.

[19] S. Pan, S. Wenzhong, H. Pengfei, H. Ming, and Z. Xiaokang, Novel approach to unsupervised change detection based on a robust semi-supervised FCM clustering algorithm, *Remote Sensing*, *8*(3), 2016, 264.

[20] J. Chunyang, L. Weihua, and L. Xiaochun, High-resolution remote sensing image segmentation based on weight adaptive fractal net evolution approach, *Remote Sensing for Land & Resources*, *25*(4), 2013, 22–25.

[21] C. Qihao, L. Linlin, X. Qiao, Y. Shuai, S. Xuguo, and L. Xiuguo, Multi-feature segmentation for high-resolution polarimetric SAR data based on fractal net evolution approach, *Remote Sensing*, *9*(6), 2017, 570.

[22] M. Lingkui, D. Ting, and Z. Wen, Drought monitoring using an Integrated Drought Condition Index (IDCI) derived from multi-sensor remote sensing data, *Natural Hazards*, *80*(2), 2016, 1135–1152.

[23] Z. Junjie, D. Xiaoping, F. Xiangtao, and G. Huadong, A advanced multi-scale fractal net evolution approach, *Remote Sensing Technology and Application*, *29*(2), 2014, 324–329.

[24] S. Tengfei, Efficient paddy field mapping using Landsat-8 imagery and object-based image analysis based on advanced fractel net evolution approach, *GI Science & Remote Sensing*, *54*(3), 2017, 354–380.

[25] M. Kai, W. Jihua, C. Zehua, Z. Xiaobo, and P. Ligang, A method for extending the geostatistical functions in spatial information processing, *Intelligent Automation and Soft Computing*, *22*(2), 2016, 261–266.

[26] S. Peirong, C. Yongfu, H. Liu, and W. Yunhua, Selection of multi-scale segmentation parameters based on segmentation evaluation function, *Remote Sensing Technology and Application*, *33*(4), 2018, 628–637.

[27] J. Luyuan, X. Pengfeng, F. Xuezhi, L. Yun, and Z. Liujun, Assessment of large-scale land cover datasets in typical areas of china based on sub-fractional error matrix, *Remote Sensing Technology and Application*, *30*(2), 2015, 353–363.

Biographies

Yang Wugu is a graduate student in College of Information and Computer, China Three Gorges University. He is currently involved in the studies of remote sensing image processing.

Tian Weixin is an Associate Professor in Computer and Information Technology School, China Three Gorges University. His research interests are data mining, intelligent algorithm and intelligent information processing.

Ming Lei is a graduate student in College of Information and Computer, China Three Gorges University. Her research direction is remote sensing image target classification.